The Cryosphere Discuss., 7, 743–788, 2013
www.the-cryosphere-discuss.net/7/743/2013/
doi:10.5194/tcd-7-743-2013

The Cryosphere Discussions
Open Access

Sensitivity of lake ice regimes to climate change in the nordic region

S. Gebre, T. Boissy, and K. Alfredsen

Department of Hydraulic and Environmental Engineering, Norwegian University of Science and Technology 7491, Trondheim, Norway

Received: 30 January 2013 – Accepted: 10 February 2013 – Published: 4 March 2013

Correspondence to: S. Gebre (solomon.gebre@ntnu.no, solomongbr@yahoo.com)

Published by Copernicus Publications on behalf of the European Geosciences Union.

Abstract

A one-dimensional process-based multi-year lake ice model, MyLake, was used to simulate lake ice phenology and annual maximum lake ice thickness for the Nordic region comprising Fennoscandia and the Baltic countries. The model was first tested and validated using observational meteorological forcing on a candidate lake (Lake Atnsjøen) and using downscaled ERA-40 reanalysis data set. To simulate ice conditions for the contemporary period of 1961–2000, the model was driven by gridded meteorological forcings from ERA-40 global reanalysis data downscaled to a 25 km resolution using the Rossby Center Regional Climate Model (RCA). The model was then forced with two future climate scenarios from the RCA driven by two different GCMs based on the SRES A1B emissions scenario. The two climate scenarios correspond to two future time periods namely the 2050s (2041–2070) and the 2080s (2071–2100). To take into account the influence of lake morphometry, simulations were carried out for four different hypothetical lake depths (5 m, 10 m, 20 m, 40 m) placed at each of the 3708 grid cells. Based on a comparison of the mean predictions in the future 30 yr periods with the control (1961–1990) period, ice cover durations in the region will be shortened by 1 to 11 weeks in 2041–2070, and 3 to 14 weeks in 2071–2100. Annual maximum lake ice thickness, on the other hand, will be reduced by a margin of up to 60 cm by 2041–2070 and up to 70 cm by 2071–2100. The simulated changes in lake ice characteristics revealed that the changes are less dependent on lake depths though there are slight differences. The results of this study provide a regional perspective of anticipated changes in lake ice regimes due to climate warming across the study area by the middle and end of this century.

1 Introduction

According to the European Environmental Agency (EEA), there are more than 500 000 natural lakes larger than 0.01 km^2 (1 ha) in Europe, and three quarters of the lakes are located in Norway, Sweden, Finland and the Karelo-Kola part of Russia (EEA database, 2012). In Northern Europe, most lakes are characterized by extended periods of winter ice cover each year (Blenckner et al., 2010). The ice season can be up to seven months long and the thickness of the ice can reach 100 cm (Leppäranta, 2010). Lake ice phenology (ice-on date, ice-off date and ice cover duration) and ice thickness are regarded as a good proxy for past and present climate (Magnuson et al., 2000); and in some cases can be considered a more robust measure of climate variability and change than air temperature (Livingstone, 1997). The various forms and processes of freshwater ice such as lake ice phenology and ice thickness are directly controlled by atmospheric conditions that influence the radiative, sensible and latent heat fluxes (Dibike et al., 2012) and hence their spatial and temporal trends can be used as indicators of climate variability and change (Prowse et al., 2011). Changes in lake ice cover characteristics due to anthropogenic causes will have significant ecological, hydrological, and socio-economic impacts (Prowse et al., 2011). This concern has increased since analysis of historical lake-ice observations indicates significant changes in the timing and duration of the ice season that is commensurate with global warming. Magnuson et al. (2000) investigated the freeze-up and break-up trends for 26 rivers and lakes in the Northern Hemisphere. Accordingly, from 1846 to 1995, average freeze-up dates were delayed by 0.58 days per decade, while break-up occurred 0.65 days earlier per decade. (Benson et al., 2012) updated the study by Magnuson et al. with more lakes and more recent data (1855–2005) and found that freeze-up occurred 0.3–1.6 days later per decade whereas break-up occurred 0.5–1.9 days earlier per decade.

Climatic variables that are used to compute the heat balance on a lake surface (temperature, precipitation, relative humidity, wind speed, cloudiness and air pressure) are strongly affected by climate change. Temperature is the most important factor of all influencing the thermal structure and ice cover regime of lakes. The magnitude of regional climate change signals varies depending on the chosen general circulation models (GCMs). The general trend however is that high-latitude regions will experience greater temperature increases than elsewhere and that these changes are likely to occur ever faster because of the positive feedback effects of melting snow and ice (Quesada et al., 2006; MacKay et al., 2009). Projections from GCMs have coarse spatial resolution (~100 km at best), and these projections are particularly inappropriate for lakes which are highly dynamic and respond in complex ways to short-term changes in weather (Samuelsson, 2010). Hence, GCM projections shall be downscaled to higher spatial resolutions (25 km or less) to capture the spatial variability in meteorological forcing. The ENSEMBLES project is one such initiative which was supported by the European Commission's 6th Framework Programme as a 5 yr Integrated Project from 2004–2009. One of the objectives of the ENSEMBLES project was to develop an ensemble prediction of climate change using high resolution regional climate models (RCMs) (van der Linden and Mitchell, 2009).

Several 1-D thermodynamic lake-models have been developed over the years, such as the Dynamic Reservoir Simulation Model – DYRSMICE (Gosink, 1987), Minnesota Lake Model – MINLAKE (Stefan and Fang, 1997), Lake Ice Model Numerical Operational Simulator – LIMNOS (Walsh et al., 1998), Canadian Lake Ice Model – CLIMo (Duguay et al., 2003), Multi-year Lake Simulation Model – MyLake (Saloranta and Andersen, 2007), and Freshwater Lake model – FLake (Mironov, 2008). The models have been successfully applied to evaluate the influence of climate and lake depth on the lake thermodynamic balance and ice-phenology. There have been, for example, quite a number of studies of model applications to characterize at-site lake ice conditions (e.g. MacKay et al., 2009; Fang et al., 1996). A number of studies have also used 1-D lake models for assessing the impact of anticipated climate change on lake thermal regimes (Fang and Stefan, 1999, 2009; Stefan et al., 1998; Saloranta et al., 2009), and ice cover characteristics (Fang and Stefan, 1998, 2009; Stefan and Fang, 1997).

The coupling of 1-D lake-models and gridded climate data over large areas is quite a recent phenomenon. Walsh et al. (1998) used a modified version of the lake-ice model LIMNOS and produced ice phenology over the Northern Hemisphere on a 0.5° by 0.5° latitude-longitude grid for the period 1931–1960. The study was conducted on hypothetical lakes with mean depths of 5 m and 20 m using average monthly climate data as input. Some studies have reported modeling results of future lake ice conditions using deterministic, process based models with input forcing from GCMs or RCMs. Dibike et al. (2012) examined possible changes to the lake ice regime in North America from 40° N to 75° N under future climate. They found that break-up will advance by 10–20 days, while freeze-up will be delayed by 5–15 days, resulting in a reduction of the ice cover duration by 15–35 days in 2041–2070 compared to 1961–1990 under the SRES A2 Scenario. Dibike et al. (2011) carried out a similar exercise, but now for the whole of the Northern Hemisphere between 40° N and 75° N (excluding Greenland), and came up with a similar conclusion: lake-ice freeze-up timing will be delayed by 5–20 days and break-up will be advanced by approximately 10–30 days, thereby resulting in an overall decrease in lake-ice duration by about 15–50 days, for the period 2040–2079 compared with 1960–1999. Brown et al. (2011) carried out a grid-based simulation of lake ice conditions for Arctic North America above 58° N and found that projected changes to the ice cover using the 30-yr mean data between 1961–1990 and 2041–2070 suggest a shift in break-up and freeze-up dates for most areas ranging from 10–25 days earlier (break-up) and 0–15 days later (freeze-up).

Hitherto, no detailed physically based modeling of lake-ice conditions has been carried out at a spatially high resolution over the Nordic region and the Baltic countries which is the focus of this study. The objective of this research is to evaluate the sensitivity of lake ice conditions to climate change in the future in the study region, particularly focusing on ice formation, break-up, duration of the ice cover and maximum annual ice thickness. Through grid based modeling of four different hypothetical lake depths (5 m, 10 m, 20 m and 40 m) applied to a 25 km spatial resolution, this study is meant to give an indication of the anticipated changes in the future and compare the results with previous large scale assessments.

2 Model description

The lake model used is MyLake (Multi-year simulation model for Lake thermo- and phytoplankton dynamics) which is a one dimensional process-based model. It simulates at a daily time step the vertical distribution of lake-water temperature, evolution of seasonal lake-ice and snow cover thickness and phosphorus-phytoplankton dynamics (Soloranta and Andersen, 2007). The most important physical, chemical, and biological processes are included in a relatively simple and transparent model structure which is coded in Matlab. MyLake was designed to be an investigative tool with a short runtime, allowing the simulation of a large number of lakes and over long periods. The model has been described previously in the literature (Soloranta and Andersen, 2007; Dibike et al., 2011, 2012), and hence we only include a brief description hereunder.

The model includes computational methods for simulating heat transfer at the air–water interface, advective heat transfer of inflow and outflow, and the internal vertical diffusion of thermal energy. The vertical profile of the lake is conceptualized as horizontal layers of equal height (ΔZ), each of them having a defined area and hence volume. The one-dimensional heat conservation equation for the temperature distribution in a horizontally homogeneous, vertically stratified lake is solved in each layer. The equation can be written as (Saloranta and Andersen, 2007):

$$A\frac{\partial T}{\partial t} = \frac{\partial}{\partial z}\left[KA\frac{\partial T}{\partial z}\right] + A\frac{H^*}{\rho_w c_p} \tag{1}$$

where T is laterally averaged water temperature [°C], K is the vertical diffusion coefficient [$m^2\,d^{-1}$], H^* is the net local heating rate (net heat flux) [$J\,m^{-2}\,d^{-1}$], A is surface area of a particular element [m^2], z is the depth from the water surface [m], t is time [days], c_p is the specific heat capacity of water [$J\,kg^{-1}\,°C^{-1}$] and ρ_w is the density of

TCD
7, 743–788, 2013

water [kg m^{-3}]. While T, K, and H^* are functions of depth (z) and time (t), A is a function of depth alone.

The vertical diffusion coefficient K, which quantifies the turbulent mixing between adjacent layers, is calculated on the basis of the stability frequency (Hondzo and Stefan, 1993):

$$N^2 = \frac{g}{\rho_w}\left(\frac{\partial \rho_w}{\partial z}\right); K = a_k (N^2)^{-0.43} \quad (2)$$

Where $a_k = 0.00706(A_s)^{0.56}$, A_s being the lake surface area in km^2.

For the top layer of the lake the net surface energy flux is calculated as:

$$H^* = H_{SW} + H_{LW} + H_{Sen} + H_{Lat} + H_{Sed} \quad (3)$$

Where H_{SW} is the incoming solar radiation absorbed by the layer, H_{LW} is the net longwave radiation, H_{Sen} and H_{Lat} are the sensible and latent heat fluxes and H_{Sed} is the heat flux at sediment-water interface (all in J m^{-2} d^{-1}). For the subsurface layers, only H_{SW} and H_{Sed} contribute to the local heating rate H^*. During the ice cover period only the sediment water flux and the shortwave radiations penetrating through snow and ice contribute to the local heating. In order to compute all these fluxes the following daily meteorological variables should be provided as input series: air temperature at 2 m height (°C), cloud cover (0–1), relative humidity (%), solar radiation (J m^{-2} d^{-1}), wind speed at 10 m height (m s^{-1}), air pressure at station level (hPa) and precipitation (mm d^{-1}).

If solar insolation observations are not available, MyLake computes H_{SW} using the MATLAB Air–Sea Toolbox as a function of Julian day, latitude and longitude (for details refer to eg. Dibike et al., 2011). The Air–Sea Toolbox is also used for the calculation of the radiative and turbulent heat fluxes, and surface wind stress. Wind has a strong influence on the lake thermal stratification in open water period. Due to the wind stress the surface water is forced to move. Depending of the wind strength, this movement is transmitted to the underlying water layers until a certain depth. In MyLake the total kinetic energy TKE (J) accumulated over one time step of 24 h (Δt = 86 400 s), available for wind-induced mixing in open water period is calculated by:

$$\mathrm{TKE} = W_{\mathrm{str}} A_{\mathrm{s}} \sqrt{\frac{\tau^3}{\rho}} \Delta t \tag{4}$$

Where τ is wind stress (N m^{-2}) calculated from the input wind speed using the MATLAB Air–Sea Toolbox. W_{str} is a wind sheltering coefficient which is calculated using the empirical relationship developed by Hondzo and Stefan (1993):

$$W_{\mathrm{str}} = 1.0 - \exp(-0.3 A_{\mathrm{s}}) \tag{5}$$

The model triggers ice formation when water layer temperature drops below the freezing point and the temperature of the super-cooled layers is set to the water freezing point. The sensible heat deficit in the super-cooled layer is turned into a latent heat of freezing and an initial ice-layer is created. However, this ice is defined as frazil ice. Before the formation of an ice-cover, ice-crystals are suspended in the water column and grow until they float to the surface and form a slushy layer which freezes to form the initial ice-cover. The thickness of frazil ice increases whenever new super-cooled water is encountered, and decreases whenever the water column receives heat to melt the frazil ice. The initial solid ice-cover, associated to the freeze-up date predicted by the model, only appears when the accumulation of frazil ice reaches a threshold thickness of 3 cm. Once a solid ice cover has been formed, additional ice thickness due to congelation ice growth is calculated whenever the air temperature T_{a} (°C) is below the freezing point using Stefan's law (Leppäranta, 1993).

$$h_{\mathrm{ice\_new}} = \sqrt{h_{\mathrm{ice}}^2 + \frac{2\kappa_{\mathrm{ice}}}{\rho_{\mathrm{ice}} L}(T_f - T_{\mathrm{ice}})\Delta t} \tag{6}$$

where κ_{ice} ($W\,°C^{-1}\,m^{-1}$) is the thermal conductivity of ice, ρ_{ice} ($kg\,m^{-3}$) the density of ice, L ($J\,kg^{-1}$) the latent heat of freezing, Δt (s) the daily time step. When the weight of snow cover exceeds the buoyancy capacity of the ice layer, the ice surface submerges and water floods on the top of ice. This water mixes with the lower layer of the snow cover and forms a slush and becomes "white-ice" (also called "snow-ice") when it freezes. White-ice formation is modeled using Eq. (7), which essentially makes the assumption that there is isostatic balance and that free water pathways always exist. The water-soaked snow layer is assumed to be compacted directly to the density of ice, and hence turned into a white-ice layer. The thickness of a new white-ice is computed as:

$$\Delta h_{si} = \max\left[0, h_{ice}\left(\left(\frac{\rho_{ice}}{\rho_w}\right) - 1\right) + h_{s\_weq}\right] \tag{7}$$

where h_{s_weq} is the thickness of the snow layer in water equivalents. White-ice properties are assumed to be the same as congelation ice, and thus the newly formed white-ice layer is subtracted from the snow cover and added to the ice layer.

Lake ice decay or melt is computed by considering the net heat flux at the air–snow or air–ice interface. The net heat flux is used to melt the snow cover first before ice melt starts. The formulation for melt (snow and ice) is given as:

$$\mathrm{melt}_{i,s} = \max\left[0, \frac{(1 - A_{coeff}) \cdot H_{SW} + H_{LW} + H_{SL}}{\rho_{i,s} \cdot L_{i,s}}\right] \tag{8}$$

Where i and s refer to snow and ice, A_{coeff} is the ice/snow attenuation coefficient, H_{SW} is the net short wave radiation, H_{LW} is the net long wave radiation, H_{SL} is the net sensible and latent heat flux, $\rho_{i,s}$ is the density of ice/snow and $L_{i,s}$ is the latent heat of ice/snow. For computing the net shortwave radiation, H_{SW}, snow and ice albedo are assigned default values of 0.77 and 0.30, respectively.

The model also takes into account lake inflows and outflows. The inflow either flows over the reservoir surface if the inflow density is less, or plunges beneath the surface if the inflow density is greater, i.e. river inflow is added to the top of the first water layer heavier than the inflow. The water column above the inflow level is then lifted up according to the volume of the inflowing water. Outflow from a lake occurs at the surface when the water level exceeds the lake surface elevation. Hence, the part of the water column that is lifted above the lake surface level (assumed to be constant) is considered as the outflow and thus lost from the lake.

3 Data and methods

3.1 Model testing

The Lake Ice Model, MyLake (Saloranta and Andersen, 2007) was first tested and validated using in situ observations on Lake Atnsjøen in south-central Norway (Fig. 1) which has long-term measured temperature profiles and ice phenology data. The model requires daily average input data for six meteorological variables, including 2 m air temperature (°C), precipitation (mm), 2 m relative humidity (percent), 10 m wind speed ($\mathrm{m\,s^{-1}}$), surface air pressure (hPa) and cloud cover (–). The short wave radiation ($\mathrm{W\,m^{-2}}$) reaching the surface is computed within the model as a function of solar altitude and cloud cover. The meteorological data at nearby stations (within a distance of 20–40 km) were obtained from the Norwegian Meteorological Institute (DNMI). Daily inflows to the lake and inflow temperatures are also required to produce an accurate thermodynamic simulation of the lake profile. Outflows are computed within the model based on daily water balance and a fixed maximum water surface elevation. Finally we need to input initial temperature profile, ice and snow thicknesses. Typically simulations start in the ice and snow free season and these values are set to zero. Inflow discharge and temperature, lake temperature profiles, and ice phenology data were obtained from the Norwegian Water Resources and Energy Directorate (NVE). The model simulates a number of lake characteristics, notably water temperature profile, freeze-up and breakup dates as well as ice and snow thicknesses. Model parameters are either

TCD
7, 743–788, 2013

fixed (e.g. $dz = 1$ m, snow albedo = 0.77, ice albedo = 0.30) or computed from lake surface areas (e.g. vertical heat diffusivity coefficient (K), and wind sheltering coefficient (W_{str})). Sensitivity analyses for model boundary conditions (input meteorology), model parameters, and initial conditions are all important tasks in model applications. In this study, we considered only model sensitivity to input meteorology and hydrology, as model parameters were left to default values and no calibration was carried out. The sensitivity analysis involves changing one variable at a time and by applying global perturbations of ±10 %, ±20 % and ±30 % on each input variable and evaluating the changes in the mean values of freeze- and break-up dates. The Atnsjøen Lake model was also driven with the RCA downscaled reanalysis data to evaluate how well the observed lake temperature and ice characteristics are reproduced.

Forcing data for the regional simulation was obtained from the online data portal of the EU ENSEMBLES project (http://ensemblesrt3.dmi.dk/), maintained at the Danish Meteorological Institute. The control period (1961–1990) lake ice conditions were simulated using the ERA-40 global re-analysis data (Uppala et al., 2005) dynamically downscaled to a 25 km resolution by using the the Rossby Centre Regional Climate Model (RCA) developed by the Swedish Meteorological and Hydrological Institute. ERA-40 is a re-analysis of meteorological observations produced by the European Centre for Medium-Range Weather Forecasts (ECMWF) and integrates measurements of varying accuracy from a wide variety of in situ and remote sensing instruments to produce a comprehensive global data set of climate data for the period 1957–2002 at 2.5° spatial resolution (Uppala et al., 2005). RCA is a coupled regional climate model which has been developed at SMHI to perform optimally in a spatial resolution range of 10 to 50 km. The model was originally developed from the high resolution weather prediction model HIRLAM, however, the majority of the physical parameterization schemes have been replaced or substantially developed to allow for accurate operation of the model in climate mode (Jones et al., 2004). A comparison of RCA output driven by ERA-40 boundary conditions and a high quality observational data set from the Climate Research Unit (CRU) showed that the model provides an accurate simulation

TCD
7, 743–788, 2013
Sensitivity of lake ice regimes to climate change
S. Gebre et al.

of the seasonal and inter-annual evolution of the near-surface temperature in Europe in general and the Nordic region in particular (Jones et al., 2004). Hence, the model results based on the re-analysis data are believed to represent the seasonal evolution of lake temperature profile and ice cover growth and ablation. In addition, as our main objective is to look at changes in ice regimes, it is expected that the effects of the biases in meteorological forcings will cancel out when considering differences in simulated lake ice characteristics.

Hypothetical lakes of 5 m, 10 m, 20 m and 40 m depths were placed at every grid cell (25 × 25 km) which gave 3708 grid cells over the study area; and MyLake simulations were carried out for every grid cell and the respective lake depths. The four hypothetical depths considered are thought to represent a large percentage of the lakes in the region and show the variation of anticipated changes with lake depths. The gridded control period simulation was also compared with historical lake ice observations (with lakes of similar depth) from the Global Lake and River Ice Phenology Database maintained at http://nsidc.org/data/lake_river_ice/ (Benson and Magnuson, 2000) which are shown in Fig. 1. In addition linear trends in simulated (using the downscaled ERA-40 reanalysis data set) lake ice phenology (freeze-up and breakup dates, and ice cover duration) as well as annual maximum lake ice thickness for the contemporary period of 1961–2000 are determined at each grid cell via linear regression.

To evaluate the agreement between measured and simulated values, two basic statistical measures of accuracy have been used as appropriate: the mean absolute error (MAE) and the mean bias error (MBE) where:

$$\mathrm{MAE} = \frac{1}{n}\sum |P_i - O_i| \tag{9}$$

$$\mathrm{MBE} = \frac{1}{n}\sum P_i - O_i = \overline{P} - \overline{O} \tag{10}$$

Where P_i and O_i are respectively predicted and observed values. The MAE measures the average magnitude of the errors in a set of forecasts without considering the signs, and hence is unambiguous and the most natural measure of average error magnitude

TCD
7, 743–788, 2013

(Fekete et al., 2004; Willmott and Matsuura, 2005). Hence, it is the average over the "total error" that is obtained by summing the absolute values of the errors where all the individual differences are weighted equally in the average. The MBE, on the other hand, is usually intended to indicate average model "bias"; that is, average over- or under-prediction and can convey useful information in relation to model performance (Fekete et al., 2004). A negative value translates to the model systematically over predicting and a positive value means the reverse.

3.2 Future scenario modeling

The future climate corresponding to the Inter-Governmental Panel on Climate Change (IPCC) SRES A1B scenario (Nakiæenoviæ and Swart, 2000) was derived from two different GCMs (ECHAM5, Max Planck Institute, GERMANY; HadCM3Q3, Hadley Center, UK) downscaled using the RCA RCM at 25 km resolution. The two GCMs were chosen because of their wide application in various climate change impact studies in the Nordic region (Bergström et al., 2007; Beldring S et al., 2006). The SRES A1 group represents a future world of very rapid economic growth, global population that peaks in mid-century and declines thereafter, and the rapid introduction of new and more efficient technologies (IPCC, 2001). The SRES A1B scenario describes a technological emphasis leading to a balance across all sources of energy. This emissions scenario was the one chosen in the EU funded ENSEMBLES project for inter-comparison of RCMs which is the source of forcings data for this study. For brevity and also since air temperature is the most important climate variable influencing freshwater ice evolution, we have presented seasonal delta changes in 2 m air temperature for the two GCMs used in the study in Fig. 2. The mean annual increase in temperature for 2041–2070 is between 1.5 °C to 3.0 °C for ECHAM5 GCM whereas HadCM3Q3 gives a warming between 2.0 °C and 4.4 °C. For the 2080s ECHAM5 gives a warming range of between 2.2 °C and 4.7 °C, whereas the corresponding increase for HadCM3Q3 lies in between 2.8 °C and 5.7 °C. Based on the seasonal distribution of the mean change signals (Fig. 2 it can be seen that the warming is much more intensive during the winter (DJF) season.

The delta-change approach using mean monthly delta changes was used to perturb the control period meteorological data using the mean monthly climate change signals. The delta-change method is simple to implement and has been widely applied in climate impact research worldwide (Lawrence and Hisdal, 2011; Teutschbein and Seibert, 2010; Hay et al., 2000). Climate models commonly exhibit biases in simulating present-day climate. To minimize the influence of biases on estimates of future impacts of climate change, it is recommended to use the delta-change approach (Jylhä et al., 2004). The method assumes that future model biases for both mean and variability will be the same as those in present-day simulations (Bader, 2008). As our main objective is to look at mean changes in ice and thermal regimes rather than extremes, the delta-change approach is well suited for the task. Monthly delta changes Δ_m, (in °C for temperature and in per cent for the five other elements) are derived as the difference between the mean monthly values for modelled 30 yr future climate and the ones for the current climate (1961–1990). The daily values for the future climate for an element X are then computed as:

$$X_{i,m}(\text{Future}) = X_{i,m}(1961\text{–}1990) + \Delta_m \qquad (11)$$

$$X_{i,m}(\text{Future}) = X_{i,m}(1961\text{–}1990) \times \left(1 + \Delta_{\frac{m}{100}}\right)(11) \qquad (12)$$

Where i is the day number and m is the month. Equation (11) is used for air temperature, and Eq. (12) is used for the other five elements. A smoothing routine according to (Sheng and Zwiers, 1998) is used to eliminate sharp and abrupt changes between days at the beginning and end of each month while maintaining the mean change values of each month. In addition care was taken so that the perturbed new series lie within the physical limits of the variables (such as maximum cloud cover = 1, or maximum relative humidity = 100 %, etc.). The potential changes to lake ice regimes on a regional basis are evaluated for two time periods in the future: mid-century (2041–2070) and end of century (2071–2100) by comparing model simulations of the future periods with the control period.

3.3 Morphometry of the hypothetical lakes

We identified lakes from the Norwegian Lakes Database which have a maximum depth between 18 and 24 m (33 lakes) and between 38 and 44 m (27 lakes). These ranges of depths were chosen to represent hypothetical lakes with maximum depth of 20 m and 40 m respectively. The area-elevation maps were downloaded from Norwegian Water Resources and Energy Directorate online database (http://atlas.nve.no) and digitized to be able to extract points at 2.5 m depth interval. The relative area, $A(z)/A_s$ versus relative depth, z/z_m curves were computed, where $A(z)$ is lake area at a given depth z, z_m is the lake maximum depth, and A_s is the lake surface area. Finally the typical lake geometries were created by taking the average value of A/A_s at a given depth. MyLake computes two model parameters from lake surface area, namely, the vertical heat diffusion coefficient, K (Eq. 2) and the wind sheltering coefficient, W_{str} (Eq. 7). The median lake surface areas were computed for the two lake depth categories representing 20 m and 40 m deep hypothetical lakes as 0.52 km^2 and 1.48 km^2 respectively and used as lake surface areas. For 5 m and 10 m hypothetical lakes, the z/z_m versus $A(z)/A_s$ relationship and the lake surface area of the 20 m deep hypothetical lakes have been used. Summary of lake morphometry data for the four lake depths considered are given in Table 1.

4 Results and discussion

4.1 Model testing on Lake Atnsjøen

Detailed model tests on Lake Atnsjøen using observational data revealed that MyLake can simulate temperature profiles (Fig. 2) with good accuracy. As shown in Fig. 2, the simulation results show very small systematic bias with MBE = −0.04 °C, and a MAE of 0.76 °C. Similarly, Fig. 3 shows the comparison of observed and simulated lake ice phenology as well as lake ice thickness. Further, the simulations were also carried out using RCA downscaled ERA40 reanalysis data focussing on ice phenology and ice thickness. The modelling accuracy for freeze-up date using the two data sources (Table 2) is a MBE of −10 days (earlier) for freeze-up for both data sets. For break up, the local climate data provides a very accurate prediction (MBE = −1 day), whereas the RCA downscaled ERA40 data predicts with a MBE of +8 days. The delay in break-up using the ERA40 data can be explained in part by the cold bias of the ERA40 data compared to observed temperatures. The biases in seasonal temperatures amount to −1.6 °C for winter (DJF) and summer (JJA), −1.9 °C for spring (MAM), and −0.6 °C for autumn (SON). The overall errors of prediction as measured by the MAE are, however, in the same order of magnitude for freeze-up, break-up and ice cover duration. It is also important to note that the simulations were carried out keeping all model parameters at default values (without calibration) to ascertain the applicability of the model for region-wide simulation.

4.2 Sensitivity to meteorological and hydrological forcing

To compare the relative influence of the variation in meteorological (air temperature, precipitation, relative humidity, wind speed, cloudiness and air pressure) and hydrological (inflows and inflow temperatures) forcings, a simple sensitivity analysis that involves changing one variable at a time has been carried out. We conducted the sensitivity analysis by applying global perturbations of ±10 %, ±20 % and ±30 % on each input variable and evaluating the changes in the mean values of freeze- and break-up dates. Some of the model inputs are interdependent, and significant correlations (correlation coefficient, $r^2 > 0.30$) exist between cloud cover and relative humidity ($r^2 = 0.34$), air temperature and inflow temperature ($r^2 = 0.71$) and air temperature and inflow volume ($r^2 = 0.32$). However, these interdependencies were not taken into account during the sensitivity analysis. From the results of the sensitivity analysis (Fig. 4a, b), it can be seen that air temperature has, by far, the strongest influence on computed ice-on and

TCD
7, 743–788, 2013

ice-off dates. The relative humidity and cloudiness, which influence the heat fluxes exchanges, are the two other main influential climate factors. The inflow temperature and volume influence the lake-ice timing only to a certain degree. In addition, it can be noted that the inflow characteristics show more influence on the computed break-up dates than on the computed freeze-up dates.

4.3 Validation of the grid-based simulation

For practical reasons, the grid-based simulation of hypothetical lakes is carried out assuming the lakes to be at steady state with no inflows and outflows. The region-wide gridded simulations (using the downscaled ERA40 reanalysis data) were compared to observations at 16 sites obtained from the Global Lake and River Ice Phenology Database (GLRIPD) (Fig. 1 and Table 3). These results also proved that the model reproduces freeze-up and breakup dates reasonably well with the gridded reanalysis data, especially when considering the uncertainty in the reanalysis data as well as ice observations. Seven lakes (1–7 in Table 2) with maximum depths ranging from 19 m to 26 m were compared with the hypothetical 20 m deep lake simulations. For each ice phenology indicator, the observation was compared to the average value of the four closest RCA cells. There was in general close correspondence between simulated and observed mean freeze-up dates with MAE of 3.9 days, the predictions being earlier than the observations in all but one lake. The MAE of the predicted mean breakup date was 13.1 days, the predictions being always later than observations. Overall, RCA based simulations over-estimated the ice cover duration by 17 days. For the 9 lakes (8–16 in Table 2) used to compare the 40 m deep lake simulations, the MAE of freeze-up simulations was 5.3 days while for breakup it was 11.3 days. Overall, the mean ice cover duration is over-estimated with a MAE of 12.5 days. It must be noted that the predicted mean break-up date is always later than the observed one by an average of 13.1 days for 20 m deep lakes and 11.3 days for 40 m deep ones. Cold-biases in the downscaled ERA40 dataset may contribute a significant portion of the prediction error of breakup. In addition, lake ice observations are usually carried out near the shores of lakes and may not be representative of the lake as a whole (IPCC, 2007). Lake ice near lake shores where observations are typically carried out may breakup earlier, whereas model predictions represent ice breakup for the entire lake and this may contribute a part in the almost 2 weeks-later prediction errors. Moreover, ice events (freeze-up and break-up) are not abrupt events and require observer judgment, thus a part of the uncertainty perhaps can be assigned to the in situ observations (Latifovic and Pouliot, 2007).

Another factor we investigated was the uncertainty related to lake surface area (As) representation. Lake surface areas were parameterised as 0.52 km^2 for the 5 m, 10 m and 20 m deep lakes and 1.48 km^2 for 40 m deep lakes in the gridded simulation. These areas were determined using the median values of 60 actual lakes used to determine the shape of the lakes. We carried out the simulation for the same period (1961–2000) by using the actual surface areas (Table 2) while maintaining the shape of the lake as in the hypothetical characterization. It has been found that the observed freeze-up dates show a much stronger dependence on lake surface areas than do the break-up dates. Similar observations have been made in relation to lake depths by (Vavrus et al., 1996). Using the actual surface areas, which are much larger than the hypothetical ones, will delay freeze-up by an average of 7.4 days and breakup by an average of 2.3 days hence reducing the mean ice cover duration by 5.3 days (Fig. 5). However, the hypothetical representation of lake surface areas in the gridded simulation may not significantly affect our results especially when considering the fact that our main interest is to find an indication of the changes in lake ice conditions in the future climate. At least a significant portion of these errors are expected to cancel out when comparing the future simulations with that of the contemporary period simulations.

4.4 Contemporary trends of simulated lake ice characteristics

We performed linear trend analysis of the contemporary lake ice simulations (1961–2000) of ice phenology (freeze-up date, break-up date and ice cover duration) as well as annual maximum lake ice thickness at each of the 3708 (25 km by 25 km) grid cells. On a regional basis freeze-up shows nearly no trend (0.0 ± 0.6 days decade^{-1}) whereas breakup has shown a regional mean advance of 0.9 day earlier per decade (-0.9 ± 2.4 days decade^{-1}). The regional mean advance of breakup is slightly higher than the value reported by Magnusson et al. (2000) which was 0.63 days earlier per decade. Ice cover duration showed a weak regional trend of 0.4 days (-0.4 ± 2.9 days decade^{-1}) shorter per decade, whereas ice thickness reduced by a regional average of 1.1 cm per decade (-1.1 cm $\pm$ 2.1 cm decade^{-1}). Figure 6 shows the lake ice phenology (Julian day) and ice thickness (cm) simulations for the control period (1961–1990) for the four hypothetical lake depths.

4.5 Changes in meteorological forcing

There is considerable confidence that climate models provide credible quantitative estimates of future climate change, with the confidence being higher for some climate variables (e.g. temperature) than for others (e.g. precipitation) (Randall et al., 2007). As the dominant climatic variable influencing ice cover characteristics and lake water thermal structure is the near surface air temperature, such confidence adds to the reliability of using climate change signals for assessing future conditions. The future scenarios for the A1B emissions scenario by two GCMS (ECHAM5 and HADCM3Q3) dynamically downscaled to a 25 km resolution using the RCA RCM (from the Rossby Center in Sweden) are used in this study. The two GCMs are among a suite of GCMs used in the EU FP6 ENSEMBLES project (van der Linden and Mitchell, 2009), and have been widely used for impact studies in the Nordic region (Bergström et al., 2007; Beldring et al., 2006). The seasonal changes in temperature for the 2050s and 2080s compared to the control period of 1961–1990 are shown in Fig. 7. Even though there are differences in the magnitude of the changes, the two models are in agreement that winter warming is the highest both in the 2050s and the 2080s, and that the warming increases with latitude. The overall mean changes in the six meteorological forcings are summarized as cumulative density function (CDF) plots in Fig. 8.

TCD
7, 743–788, 2013

Title Page
Abstract | Introduction
Conclusions | References
Tables | Figures
◂◂ | ▸▸
◂ | ▸
Back | Close
Full Screen / Esc
Printer-friendly Version
Interactive Discussion

4.6 Lake ice phenology and ice thickness

Figure 9 shows expected future changes in lake ice phenology and ice thickness for mid-century (2041–2070) compared to the control period (1961–1990), and for 20 m deep lakes. Accordingly, freeze-up will be delayed by 2 to 22 days with the largest changes occurring in lower latitudes. Breakup timing, on the other hand, will advance on a larger margin of 8 to 74 days. The advance in breakup will also be larger in the lower latitudes. The delay in freeze-up and the advance in breakup will reduce the duration of ice cover by 12 to 68 days. The mean annual maximum lake ice thickness will show a marked reduction ranging from 3 cm to 59 cm and the largest diminution occurring along the Norwegian mountain ranges. The variability of the changes for various lake depths are compared as shown in Fig. 10. The changes in ice phenology and thickness don't show a clear pattern with lake depths, though there are slight variations. Figure 11 shows the changes in lake ice parameters for end-of-century (2071–2100) period. Freeze-up dates delay by between 5 and 26 days while breakup dates advance by between 11 and 73 days leading to a reduction in ice cover duration of 21 to 85 days (compared to 12 to 68 days for 2041–2070). The sensitivity of the expected changes to various lake depths is depicted in Fig. 12, which shows that the expected changes do not show clear and significant dependency with lake depths.

4.7 Lake water thermal structure

Changes in water temperature profiles are also expected as a result of the changes in meteorological forcing data. The mean annual temperature profiles were simulated for the current and the mid-century (2041–2070) future time period (average of simulations using the two GCMs chosen for the study) along a latitudinal gradient varying from 56.25° N to 66.25° N at 2° intervals and along two longitudinal axes, 15° E and 25° E. The computations were carried out for 20 m deep hypothetical lakes. The expected changes are then computed as a difference between the future and current period simulations. According to the results (as shown in Fig. 13), the summer stratification is expected to start earlier and last longer under the future climate conditions. Largest changes will arise during the open water period since when an ice cover is set-up water is isolated from the air. Consequently, southern lakes will experience changes in water temperature most of the year while changes in water temperature for northern lakes will be confined to summer and autumn. It is also observed that upper regions of the water column will have larger temperature increases than the lower regions. This will lead to generally steeper vertical temperature gradients and enhanced thermal stability similar to what has been reported by a number of other modeling studies (Hondzo and Stefan, 1993; Stefan et al., 1998; Fang and Stefan, 2009). The largest change in water temperature arises during the ice-break-up period. In fact, since under future climate condition lakes are expected to be free of ice earlier, air will be able to warm the lake surface sooner. To a smaller extent water is also cooled down slower in the autumn period. Slight decreases in water temperature during winter at the lake bottom are probably due to the reduction of the ice-cover and its insulating effect. Since the summer stratification is lasting longer, it delays the autumn turnover of the lake, that's why slight decreases in water temperature are also experienced in autumn under future climate condition.

5 Summary and conclusions

This study has examined the effects of climate change on lake ice phenology and lake ice thickness in the Nordic and Baltic regions in Northern Europe. A one-dimensional, process-based model of lake-water temperature, ice-cover growth and ablation (MyLake) was used to simulate lake ice phenology and ice thickness on a spatial grid of 25 km. The model underwent a thorough testing and validation process using a candidate lake that provided reasonable evidence that the model accurately captured the essential elements of the physical system. In addition, the grid-based simulation using downscaled ERA40 reanalysis data reasonably matched the historical variability in observational datasets from the GLRIPD database. After successful model testing and validation, the potential effects of climate change on lake-ice timing and thickness were studied with the use of modeling results based on the RCA RCM driven by two GCMs under SRES A1B emission scenario. Using climate change signals from two GCMs as opposed to just one in a number of similar studies has the advantage of addressing the uncertainties in climate projections to a certain level. Two future periods: mid-century-2041–2070 and end-of-century-2071–2100 were considered to look at medium-term and long-term changes due to perceived climate change. The results showed that freeze-up will delay by an average of 1 to 3 weeks in 2041–2070 and 1 to 4 weeks in 2071–2100. Breakup, on the other hand, will advance by between 1 to 10 weeks in 2041–2070 and by 2 to 10 weeks in 2071–2100. The combined effects of a delay in freeze-up and an advance in breakup will shorten the ice duration by 1 to 11 weeks in 2041–2070 and 3 to 14 weeks in 2071–2100. Ice thickness shows a reduction between 1 and 60 cm in 2041–2070 and 1 to 70 cm in 2071–2100. For practical reasons, the gridded simulations were carried out by assuming the lakes to be at steady state without inflows and outflows. This will exclude the effect of the expected increase in winter flows in the future climate. However, it has been shown in the sensitivity analysis of the Lake Atnsjøen application that ice phenology results are very much less sensitive to inflow volumes. For example, a 30 % global increase in inflows produced only a delay of 0.23 days in freeze-up date. Hence, it can be argued that the omission of inflows to the hypothetical lakes simulated will not alter the order of magnitude of the results reported.

We further compared our results with a large scale study of the Northern Hemisphere (we call it hemispherical study) above 40° N by Dibike at al. (2011), where they evaluated changes for the period 2040–2079 versus 1960–1999 considering 20 m deep hypothetical lakes placed at 2.5° spatial grids. The comparison is made with our simulation of the changes between the future period 2041–2070 and the control period 1961–1990. The change in freeze-up dates is closely comparable, where the hemispherical study gives changes in the order of 0 to 20 days later for our study area; whereas our study at 25 km grid shows a range from 2 to 22 days later. Break-up, on the other hand, is expected to advance by 0 to 30 days in the case of the hemispherical study; whereas in our simulation it will advance by 7 to more than 70 days. Ice thickness reduction ranged from 0 to 40 cm in the hemispherical study, whereas the present study showed values in the range of 2 to 60 cm. The comparison shows that the changes are more pronounced in the high resolution study we carried out compared to the large scale study. In addition to the spatial resolution, the studies used different climate forcing both for the contemporary period (ERA-40 data versus downscaled ERA-40 data) and for the future climate where different GCMs and RCMs have been used for input forcing for the future period. Hence, the uncertainty associated with input forcing both due to spatial resolution and differing GCM-RCM combination imparts uncertainties in the expected changes in the future.

The IPCC Working Group II, Third and Fourth Assessment Reports (Anisimov et al., 2007) have stated that there is very high confidence that components of the terrestrial cryosphere and hydrology are increasingly being affected by climate change. A number of studies have demonstrated that freshwater cryosphere and especially lake ice duration and thickness will be considerably reduced in the future (Dibike et al., 2011, 2012; Brown and Duguay, 2011; Walsh et al., 1998). Changes in thermodynamic characteristics of lakes due to diminished ice cover duration (such as the one predicted in this study) will lead to a number of physical, biological, and chemical changes (Corell and Cleveland, 2010; ACIA, 2005). Summer stratification is expected to start earlier due to the advance of breakup and last longer due to the delay in freeze-up as shown in our results. Decreases in lake-ice duration combined with higher temperatures during the increasingly long open-water period will lead to increased evaporation and lowering of lake levels (AMAP, 2011). Largest changes in water temperature are expected in the ice-free period resulting in increased evaporation from freshwater lakes. Periods that normally have ice covers will be ice free due to climate change impacts and this will increase biological activity in the lakes. A great economic impact is also likely to arise from a reduced ice thickness and bearing capacity which could restrict the size and load limit of traffic (ACIA, 2005; Prowse et al., 2011). A shorter ice season and thinner ice cover could have some desirable consequences to hydroelectric power operation. It can lead to reduced static ice loads on dams (Prowse et al., 2011), and more water could be available during winter due to reduction of immobilized water that freezes (Seidoua et al., 2007).

Climate model predictions show a consistent enhanced warming at higher latitudes, the winter season showing the larger percentage of the changes. A physics-based modeling using the change signals have shown that this enhanced warming, together with changes in other atmospheric variables, will result in a significant decline in lake ice duration and thickness at the end of the 21st century in the Nordic-Baltic region. In addition, there will also be significant changes in the thermal structure of lakes, with lakes in lower latitude warming much more than lakes in higher latitudes. These changes will have consequences to the socio-economic and ecological functions of the lakes.

Acknowledgements. This work was supported by a Ph.D. grant from the Norwegian Research Council under the Sustainable Infrastructure program through the Norwegian University of Science and Technology. The work is also supported by the Centre for Environmental Design of Renewable Energy (CEDREN) and the Cryosphere-Atmosphere Interactions in a Changing Arctic Climate (CRAICC) Project. We would like to thank Tuomo Saloranta for providing the MATLAB code of the MyLake model and additional assistance in model use. We also would like to thank Ånund Kvambekk at the Norwegian Water Resources and Energy Directorate for providing lake ice data for model validation. In addition, we thank all other data sources cited Sect. 3 of this paper.

References

AMAP: Snow, Water, Ice and Permafrost in the Arctic (SWIPA): Climate Change and the Cryosphere, Arctic Monitoring and Assessment Programme (AMAP), Oslo, Norway, 538 pp., 2011.

Anisimov, O. A., Vaughan, D. G., Callaghan, T. V., Furgal, C., Marchant, H., Prowse, T. D., Vilhjálmsson, H., and Walsh, J. E.: Polar regions (Arctic and Antarctic), in: Climate Change

TCD
7, 743–788, 2013

2007: Impacts, Adaptation and Vulnerability. Contribution of Working Group II to the Fourth Assessment Report of the Intergovernmental Panel on Climate Change, edited by: Parry, M. L., Canziani, O. F., Palutikof, J. P., v. d. Linden, P. J., and Hanson, C. E., Cambridge University Press, Cambridge, 653–685, 2007.

Benson, B., Magnuson, J., Jensen, O., Card, V., Hodgkins, G., Korhonen, J., Livingstone, D., Stewart, K., Weyhenmeyer, G., and Granin, N.: Extreme events, trends, and variability in Northern Hemisphere lake-ice phenology (1855–2005), Climatic Change, 12, 299–323, doi:10.1007/s10584-011-0212-8, 2012

Bergström, S., Jóhannesson, T., Adalgeirsdóttir, G., Andreassen, L. M., Beldring, S., Hock, R., Jónsdóttir, J. F., Rogozova, S., and Veijalainen, N.: Hydropower, in: Impacts of Climate Change on Renewable Energy Sources – Their Role in the Nordic Energy System, edited by: Fenger, J., Report Nord 2007:003, 228 pp., 2007.

Blenckner, T., Adrian, R., Arvola, L., Järvinen, M., Nõges, P., Nõges, T., Pettersson, K., and Weyhenmeyer, G. A.: The impact of climate change on lakes in Northern Europe, in: Aquatic Ecology Series, edited by: George, G., Springer Netherlands, 339–358, 2010.

Brown, L. C. and Duguay, C. R.: The fate of lake ice in the North American Arctic, The Cryosphere, 5, 869–892, doi:10.5194/tc-5-869-2011, 2011.

Dibike, Y., Prowse, T., Saloranta, T., and Ahmed, R.: Response of Northern Hemisphere lake-ice cover and lake-water thermal structure patterns to a changing climate, Hydrol. Process., 25, 2942–2953, 2011.

Dibike, Y., Prowse, T., Bonsal, B., Rham, L. D., and Saloranta, T.: Simulation of North American lake-ice cover characteristics under contemporary and future climate conditions, Int. J. Climatol., 32, 695–709, doi:10.1002/joc.2300, 2012.

Duguay, C. R., Flato, G. M., Jeffries, M. O., Ménard, P., Morris, K., and Rouse, W. R.: Ice-cover variability on shallow lakes at high latitudes: model simulations and observations, Hydrol. Process., 17, 3465–3483, doi:10.1002/hyp.1394, 2003.

Fang, X. and Stefan, H. G.: Potential climate warming effects on ice covers of small lakes in the contiguous US, Cold Reg. Sci. Technol., 27, 119–140, doi:10.1016/j.coldregions.2004.06.010, 1998.

Fang, X. and Stefan, H. G.: Projections of climate change effects on water temperature characteristics of small lakes in the contiguous US, Climatic Change, 42, 377–412, doi:10.1023/a:1005431523281, 1999.

Fang, X. and Stefan, H. G.: Simulations of climate effects on water temperature, dissolved oxygen, and ice and snow covers in lakes of the contiguous United States under past and future climate scenarios, Limnol. Oceanogr., 54, 2359–2370, doi:10.1016/j.coldregions.2004.06.010, 2009.
Fang, X., Ellis, C. R., and Stefan, H. G.: Simulation and observation of ice formation (freeze-over) in a lake, Cold Reg. Sci. Technol., 24, 129–145, 1996.
Fekete, B. M., Vörösmarty, C. J., Roads, J. O., and Willmott, C. J.: Uncertainties in precipitation and their impacts on runoff estimates, J. Climate, 17, 294–304, 2004.
Gosink, J. P.: Northern lake and reservoir modeling, Cold Reg. Sci. Technol., 13, 281–300, 1987.
Hay, L. E., Wilby, R. L., and Leavesley, G. H.: A comparison of delta change and downscaled GCM scenarios for three mountainous basins in the United States, J. Am. Water Resour. As., 36, 387–397, 2000.
Hondzo, M. and Stefan, H.: Lake water temperature simulation model, J. Hydraul. Eng.-ASCE, 119, 1251–1273, doi:10.1061/(ASCE)0733-9429(1993)119:11(1251), 1993.
IPCC: Climate Change 2001: The Scientific Basis. Contribution of Working Group I to the Third Assessment Report of IPCC, available at: http://www.ipcc.ch, 2001.
IPCC: Climate Change 2007: The Scientific Basis. Contribution of Working Group I to the Fourth Assessment Report of IPCC, available at: http://www.ipcc.ch, 2007.
Jones, C. G., Willén, U., Ullerstig, A., and Hansson, U.: The Rossby centre regional atmospheric climate model Part I: model climatology and performance for the present climate over Europe, AMBIO, 33, 199–210, doi:10.1579/0044-7447-33.4.199, 2004.
Jylhä, K., Tuomenvirta, H., and Ruosteenoja, K.: Climate change projections for Finland during the 21st century, Boreal Environ. Res., 9, 127–152, 2004.
Latifovic, R. and Pouliot, D.: Analysis of climate change impacts on lake ice phenology in Canada using the historical satellite data record, Remote Sens. Environ., 106, 492–507, doi:10.1016/j.rse.2006.09.015, 2007.
Lawrence, D. and Hisdal, H.: Hydrological Projections for Floods in Norway Under a Future Climate, NVE, Oslo, 47 pp., 2011.
Leppäranta, M.: A review of analytical models of sea-ice growth, Atmos. Ocean, 31, 123–138, doi:10.1080/07055900.1993.9649465, 1993.

Leppäranta, M.: Modelling the formation and decay of lake ice, in: The Impact of Climate Change on European Lakes, edited by: George, G., Aquatic Ecology Series, Springer Netherlands, 63–83, 2010.

Livingstone, D. M.: Break-up dates of Alpine lakes as proxy data for local and regional mean surface air temperatures, Climatic Change, 37, 407–439, doi:10.1023/a:1005371925924, 1997.

MacKay, M. D., Neale, P. J., Arp, C. D., Domis, L. N. D. S., Fang, X., Gal, G., Jöhnk, K. D., Kirillin, G., Lenters, J. D., Litchman, E., MacIntyre, S., Marsh, P., Melack, J., Mooij, W. M., Peeters, F., Quesada, A., Schladow, S. G., Schmid, M., Spence, C., and Stokes, S. L.: Modeling lakes and reservoirs in the climate system, Limnol. Oceanogr., 54, 2315–2329, 2009.

Magnuson, J. J., Robertson, D. M., Benson, B. J., Wynne, R. H., Livingstone, D. M., Arai, T., Assel, R. A., Barry, R. G., Card, V., Kuusisto, E., Granin, N. G., Prowse, T. D., Stewart, K. M., and Vuglinski, V. S.: Historical trends in lake and river ice cover in the Northern Hemisphere, Science, 289, 1743–1746, doi:10.1126/science.289.5485.1743, 2000.

Mironov, D. V.: Parameterization of Lakes in Numerical Weather Prediction – Description of a Lake Model, German Weather Service, Germany 2008.

Prowse, T., Alfredsen, K., Beltaos, S., Barrie R. Bonsal, Bowden, W. B., Duguay, C. R., Korhola, A., McNamara, J., Vincent, W. F., Vuglinsky, V., Anthony, K. M. W., and Weyhenmeyer, G. A.: Effects of changes in Arctic lake and river ice, AMBIO, 40, 63–74, doi:10.1007/s13280-011-0217-6, 2011.

Quesada, A., Vincent, W. F., Kaup, E., Hobbie, J. E., Laurion, I., Pienitz, R., López-Martínez, J., and Durán, J. J.: Landscape control of high latitude lakes in a changing climate, in: Trends in Antarctic Terrestrial and Limnetic Ecosystems, edited by: Bergstrom, D. M., Convey, P., and Huiskes, A. H. L., Springer Netherlands, 221–252, 2006.

Randall, D. A., Wood, R. A., Bony, S., Colman, R., Fichefet, T., Fyfe, J., Kattsov, V., Pitman, A., Shukla, J., Srinivasan, J., Stouffer, R. J., Sumi, A., and Taylor, K. E.: Cilmate models and their evaluation, in: Climate Change 2007: The Physical Science Basis. Contribution of Working Group I to the Fourth Assessment Report of the Intergovernmental Panel on Climate Change, edited by: Solomon, S., Qin, D., Manning, M., Chen, Z., Marquis, M., Averyt, K. B., Tignor, M., and Miller, H. L., Cambridge University Press, Cambridge, UK and New York, NY, USA, 2007.

Saloranta, T. M. and Andersen, T.: MyLake – a multi-year lake simulation model code suitable for uncertainty and sensitivity analysis simulations, Ecol. Model., 207, 45–60, doi:10.1007/s10750-007-9201-3, 2007.

Saloranta, T. M., Forsius, M., Järvinen, M., and Arvola, L.: Impacts of projected climate change on the thermodynamics of a shallow and a deep lake in Finland: model simulations and Bayesian uncertainty analysis, Hydrol. Res., 40, 234–248, doi:10.2166/nh.2009.030, 2009.

Samuelsson, P.: Using regional climate models to quantify the impact of climate change on lakes, in: The Impact of Climate Change on Lakes in Northern Europe, edited by: George, G., Aquatic Ecology Series, Springer Netherlands, 15–32, 2010.

Seidoua, O., Ouardaa, T. B. M. J., and Bilodeaub, L.: Reservoir storage loss due to grounded ice during winter operation, J. Hydrol., 335, 15–24, 2007.

Sheng, J. and Zwiers, F.: An improved scheme for time-dependent boundary conditions in atmospheric general circulation models, Clim. Dynam., 14, 609–613, doi:10.1007/s003820050244, 1998.

Stefan, H. G. and Fang, X.: Simulated climate change effects on ice and snow covers on lakes in a temperate region, Cold Reg. Sci. Technol., 25, 137–152, 1997.

Stefan, H. G., Fang, X., and Hondzo, M.: Simulated climate change effects on year-round water temperatures in temperate zone lakes, Climatic Change, 40, 547–576, doi:10.1023/a:1005371600527, 1998.

Teutschbein, C. and Seibert, J.: Regional climate models for hydrological impact studies at the catchment scale: a review of recent modeling strategies, Geogr. Compass, 4, 834–860, doi:10.1111/j.1749-8198.2010.00357.x, 2010.

Uppala, S. M., Kållberg, P. W., Simmons, A. J., Andrae, U., Bechtold, V. D. C., Fiorino, M., Gibson, J. K., Haseler, J., Hernandez, A., Kelly, G. A., Li, X., Onogi, K., Saarinen, S., Sokka, N., Allan, R. P., Andersson, E., Arpe, K., Balmaseda, M. A., Beljaars, A. C. M., Berg, L. V. D., Bidlot, J., Bormann, N., Caires, S., Chevallier, F., Dethof, A., Dragosavac, M., Fisher, M., Fuentes, M., Hagemann, S., Hólm, E., Hoskins, B. J., Isaksen, L., Janssen, P. A. E. M., Jenne, R., McNally, A. P., Mahfouf, J. F., Morcrette, J. J., Rayner, N. A., Saunders, R. W., Simon, P., Sterl, A., Trenberth, K. E., Untch, A., Vasiljevic, D., Viterbo, P., and Woollen, J.: The ERA-40 re-analysis, Q. J. Roy. Meteor. Soc., 131, 2961–3012, doi:10.1256/qj.04.176, 2005.

Vavrus, S. J., Wynne, R. H., and Foley, J. A.: Measuring the sensitivity of southern Wisconsin lake ice to climate variations and lake depth using a numerical model, Limnol. Oceanogr., 41, 822–831, 1996.

TCD
7, 743–788, 2013

Walsh, S. E., Vavrus, S. J., Foley, J. A., Fisher, V. A., Wynne, R. H., and Lenters, J. D.: Global patterns of lake ice phenology and climate: model simulations and observations, J. Geophys. Res., 103, 28825–28837, doi:10.1029/98jd02275, 1998.
Willmott, C. J. and Matsuura, K.: Advantages of the mean absolute error (MAE) over the root mean square error (RMSE) in assessing average model performance, Climate Res., 30, 79–82, 2005.

Table 1. Lake morphometric characteristics for gridded simulation.

Characteristics	Hypothetical lake depths			
Maximum depth	5 m	10 m	20 m	40 m
Mean depth	1.6 m	3.2 m	6.4 m	14.8 m
Surface area	0.52 km^2	0.52 km^2	0.52 km^2	1.47 km^2

TCD
7, 743–788, 2013

Table 2. Lake ice phenology results for lake Atnsjøen using various sources of input meteorological forcing.

	Mean (Julian date)			Mean Bias Error (days)			Mean Absolute Error (days)		
	FU	BU	ICD	FU	BU	ICD	FU	BU	ICD
Observed	329	145	197	–	–	–	–	–	–
Local climate	321	145	191	−10	−1	8	8	3	6
RCA Downscaled ERA40	316	155	205	−10	8	20	5	8	9

FU = Freeze-up date, BU = Break-up date, ICD = Ice cover duration.

TCD
7, 743–788, 2013

Table 3. Characteristics and locations of lakes used to validate grid-based lake-ice simulation using RCA downscaled ERA-40 data set (taken from GLRIPD).

No.	Lake name	Country	Lon. (deg)	Lat. (deg)	Elev. (m)	Mean Depth (m)	Max Depth (m)	Area (km^2)
1	Ala-Kintaus	Finland	25.34	62.28	154	5	19	7
2	Ala-Kivijarvi-Yla-Munni	Finland	27.51	60.94	75	5	19	92
3	Kalmarinjarvi	Finland	25.00	62.79	130	6	22	7
4	Kuortaneenjarvi	Finland	23.41	62.86	76	3	16	15
5	Naamankajarvi	Finland	28.25	65.10	174	3	14	9
6	Paajarvi-Karstula	Finland	24.81	62.86	144	4	15	30
7	Simpelejarvi	Finland	29.49	61.60	69	9	26	59
8	Hankavesi-Rautalampi	Finland	26.83	62.62	96	7	49	18
9	Kivijarvi-Saarenkyla	Finland	25.13	63.27	131	8	44	154
10	Korvuanjarvi	Finland	28.67	65.35	242	6	37	15
11	Lappajarvi-Halkosaari	Finland	23.64	63.26	70	7	39	146
12	Muurasjarvi	Finland	25.34	63.47	112	9	36	21
13	Nackten	Sweden	14.57	62.91	324	16	44	84
14	Oulujarvi	Finland	27.33	64.33	123	8	35	928
15	Rehja	Finland	27.79	64.23	138	9	42	96
16	Vesijarvi	Finland	25.54	61.18	81	7	40	108

TCD
7, 743–788, 2013

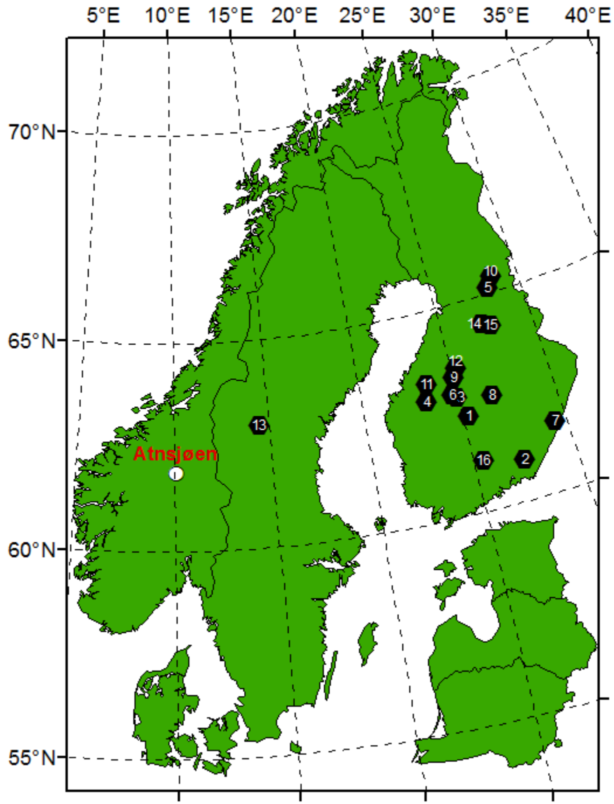

Fig. 1. Figure showing the study area domain, Lake Atnsjøen (white circle) used for detail model testing and the location of additional 16 lakes (black circles) used for validation of the gridded simulation

TCD
7, 743–788, 2013

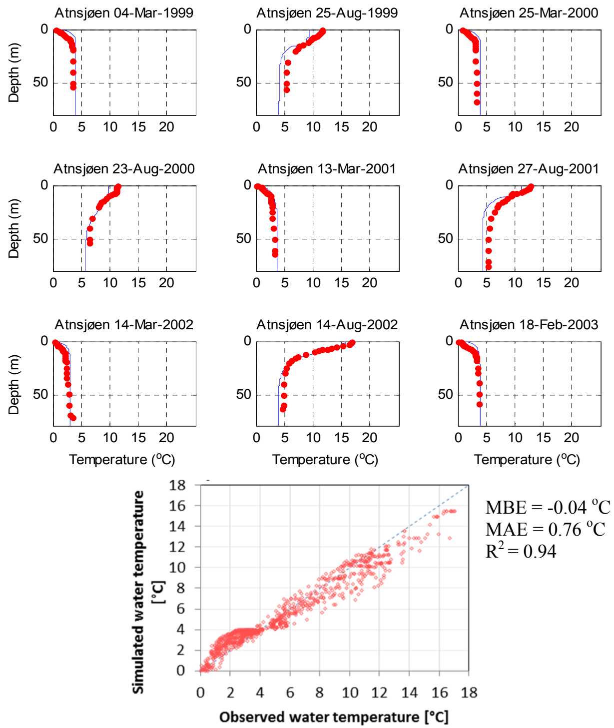

Fig. 2. A partial view of simulated (solid lines) and observed (dots) temperature profiles for Lake Atnsjøen using observational forcing data. Bottom graph shows the overall performance of the model in predicting water temperature profiles.

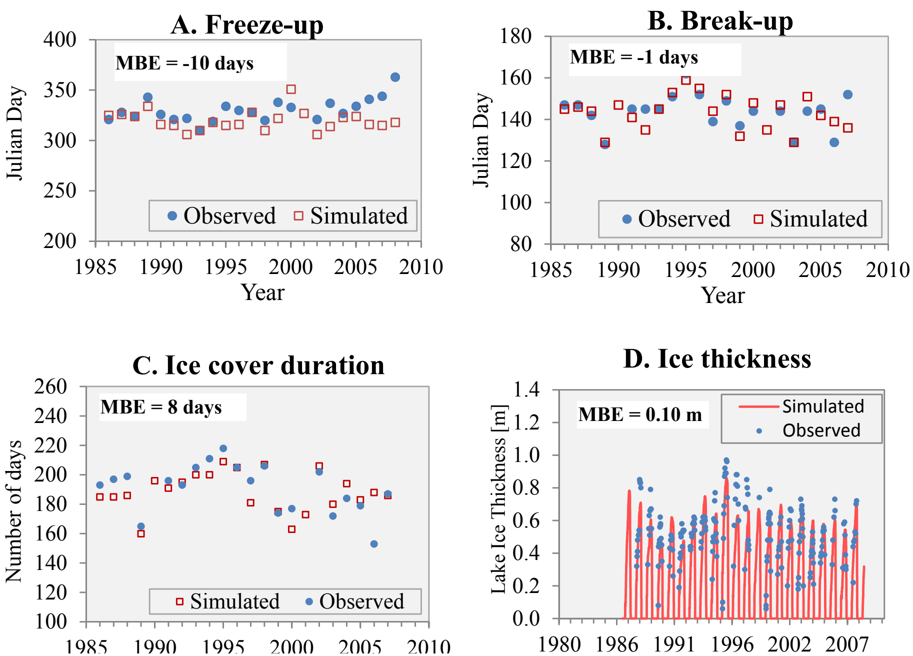

Fig. 3. Results of model tests on Lake Atnsjøen based on observed meteorological forcing data; also shown are the Mean Bias Error (MBE) values: **(A)** freeze-up date, **(B)** breakup date, **(C)** ice cover duration, **(D)** total Lake-ice thickness.

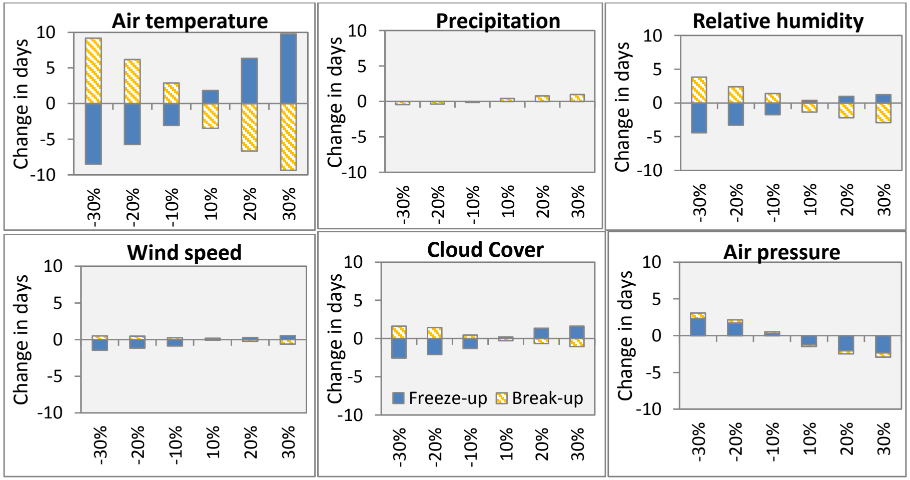

Fig. 4a. Sensitivity of ice phenology (freeze- and break-up dates) simulation results to changes in input meteorological forcing data for the case of Lake Atnsjøen. The same legend is used for all plots.

TCD
7, 743–788, 2013

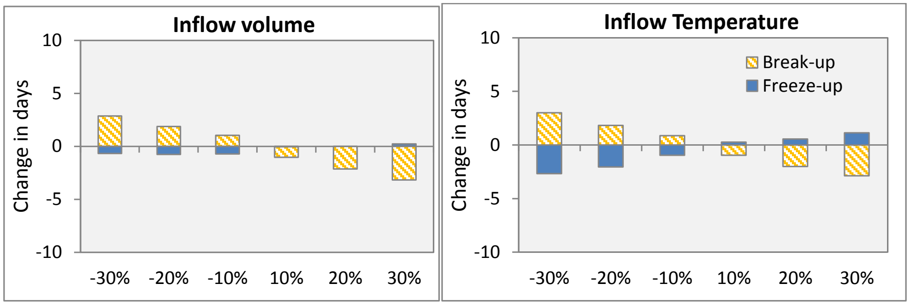

Fig. 4b. Same as Fig. 4a but to changes in input hydrological forcing data.

TCD
7, 743–788, 2013

Sensitivity of lake ice regimes to climate change

S. Gebre et al.

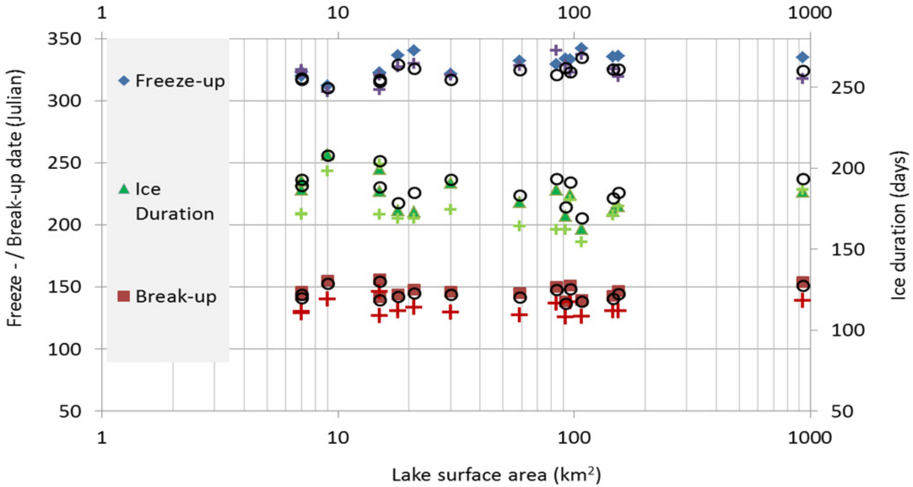

Fig. 5. Evaluation of lake ice simulation using downscaled ERA-40 gridded data set and observational data for 20 m and 40 m deep lakes (shown in Table 3); the legend shows the simulated values using actual surface areas, circles represent simulation based on the hypothetical lake characterization whereas the cross symbols are the respective observations.

TCD
7, 743–788, 2013

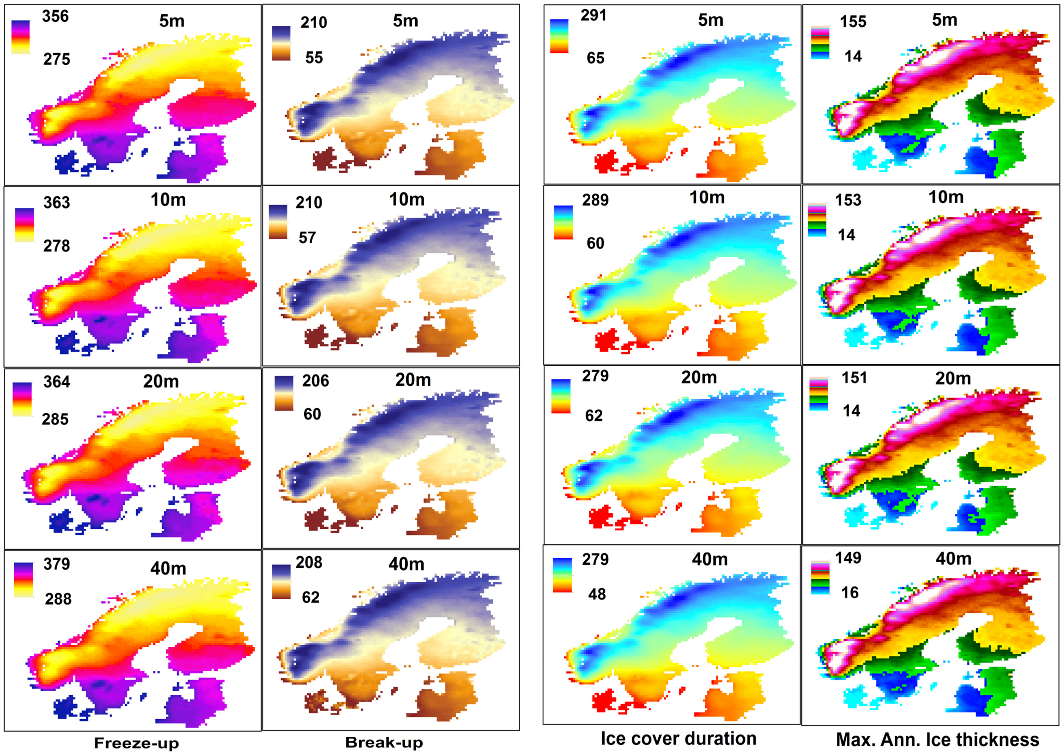

Fig. 6. Lake ice phenology (Julian day days^{-1}) and ice thickness (cm) simulation for the control period (1961–1990) for the four hypothetical lakes as simulated using dynamically downscaled ERA-40 reanalysis data with a spatial resolution of 25 km.

TCD
7, 743–788, 2013

Sensitivity of lake ice regimes to climate change

S. Gebre et al.

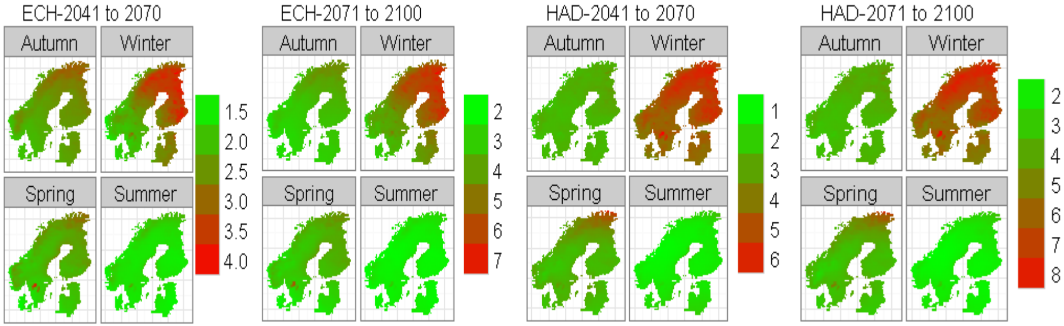

Fig. 7. Mean seasonal delta changes of 2 m air temperature for two future periods, 2050s and 2080s, compared to the standard period of 1961–1990 using downscaled data by RCA RCM from two GCMs (ECH-ECHAM5, HAD-HadCM3Q3).

TCD
7, 743–788, 2013

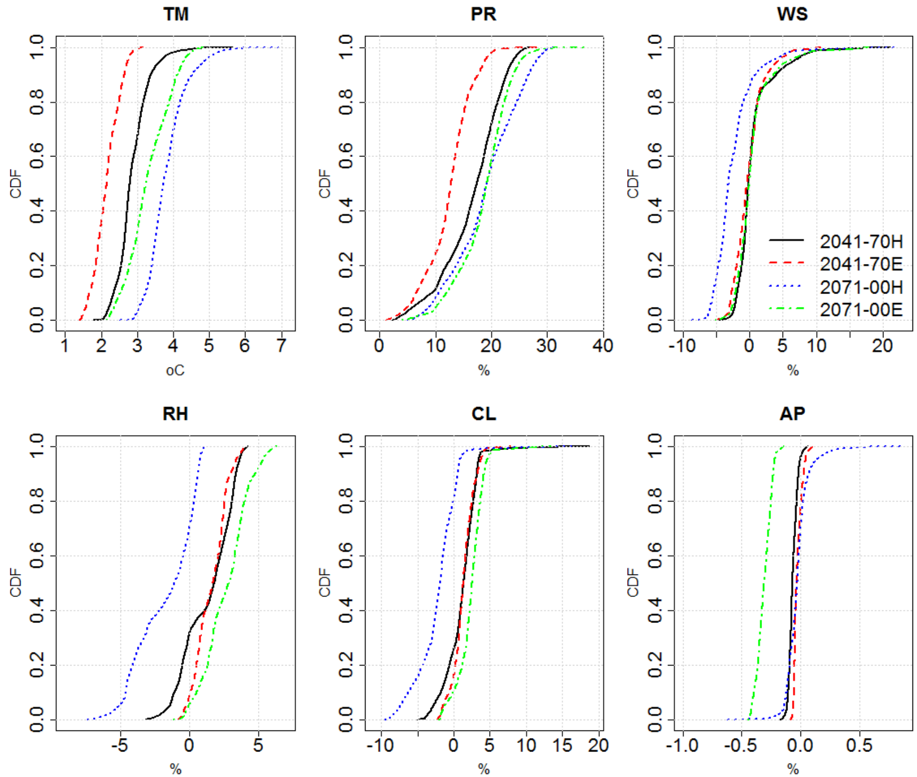

Fig. 8. Cumulative density function (CDF) plot of mean delta changes for the two future periods in the six meteorological forcings (TM = 2 m air temperature, PR = Precipitation, WS = 10 m wind speed, RH = 2 m Relative humidity, CL=total cloudiness, and AP = air pressure). The same legend is used for all plots; H refers to HadCM3Q3, and E refers to ECHAM5.

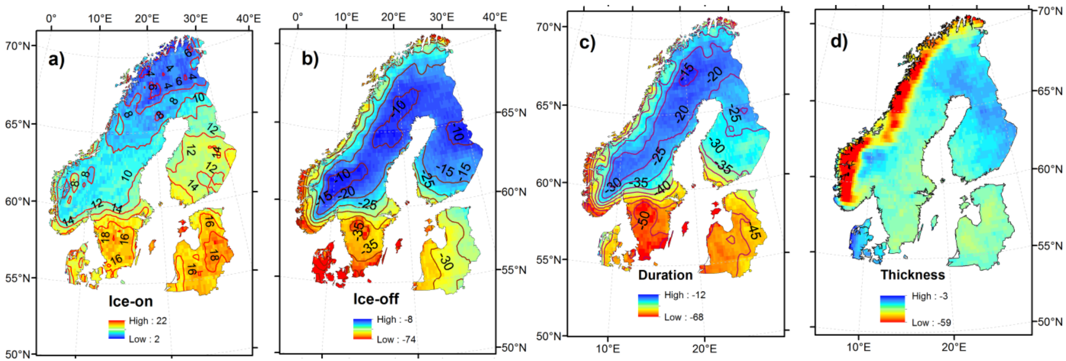

Fig. 9. Changes in future ice conditions (2041–2070) compared to the control period (1961–1990) for 20 m deep lakes: **(a)** ice-on dates, **(b)** ice-off dates, **(c)** ice duration, and **(d)** ice thickness. The results are derived from the mean simulations using the two GCMs (ECHAM5 and HadCM3Q3).

TCD
7, 743–788, 2013

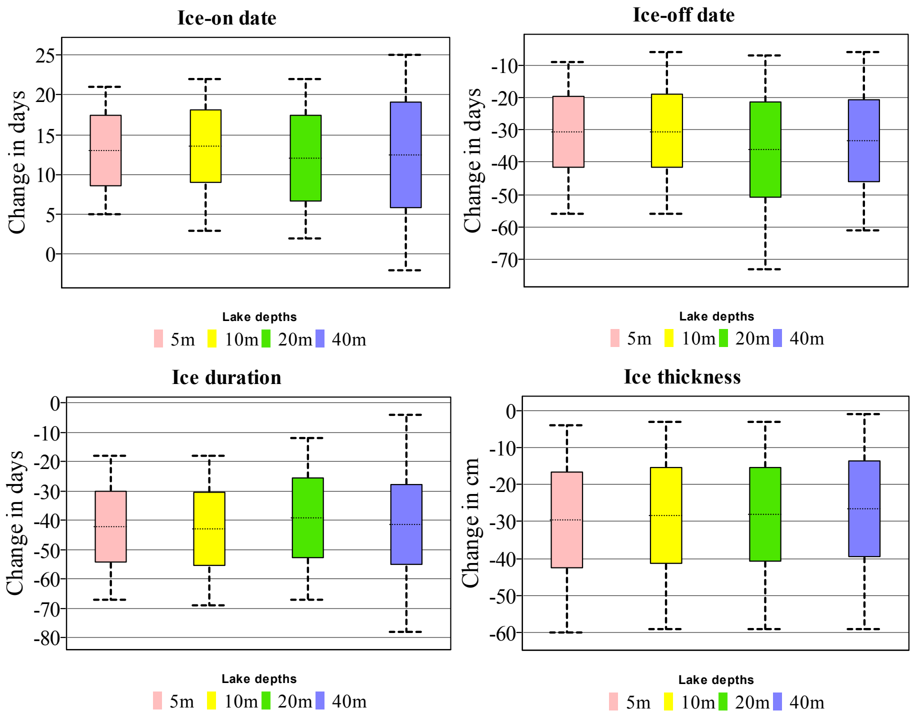

Fig. 10. Box plot showing the variability of the future changes for 2041–2070 and for various lake depths (box plots show the minimum, maximum, 25th and 75th percentile and median values).

TCD
7, 743–788, 2013

Title Page
Abstract Introduction
Conclusions References
Tables Figures
◀I ▶I
◀ ▶
Back Close
Full Screen / Esc
Printer-friendly Version
Interactive Discussion

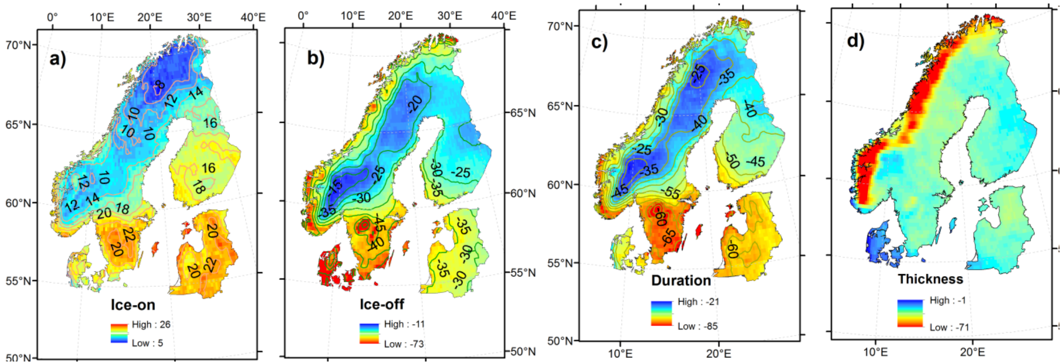

Fig. 11. Changes in future ice conditions (2071–2100) compared to the control period (1961–1990) for 20 m deep lakes: **(a)** ice-on dates, **(b)** ice-off dates, **(c)** ice duration, and **(d)** ice thickness (cm). The results are derived from the mean simulations using the two GCMs (ECHAM5 and HadCM3Q3).

TCD
7, 743–788, 2013

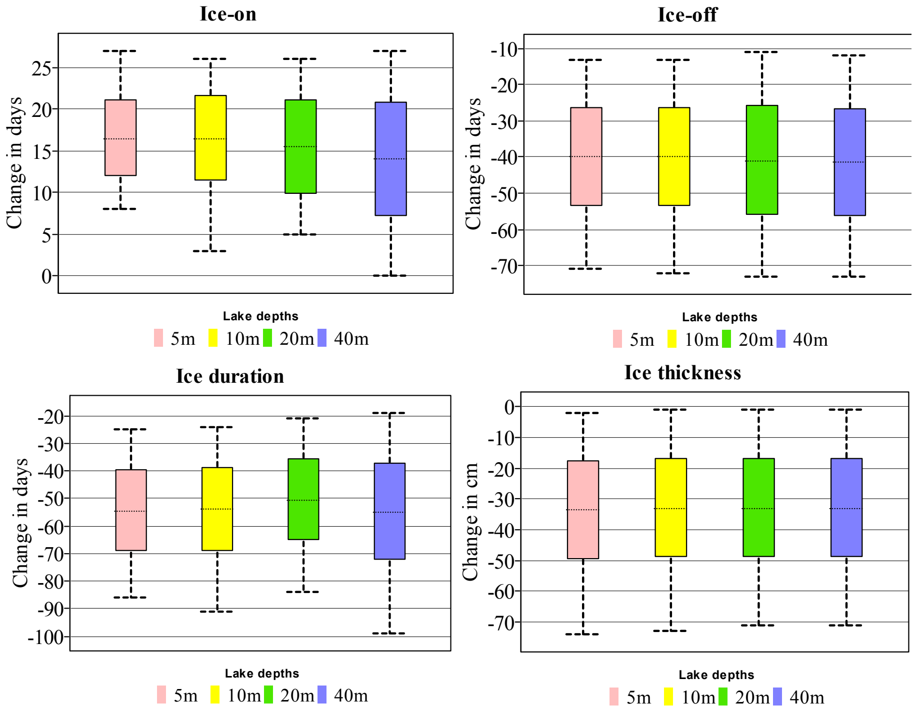

Fig. 12. Box plot showing the variability of the future changes for 2071–2100 and for various lake depths (box plots show the minimum, maximum, 25th and 75th percentile and median values).

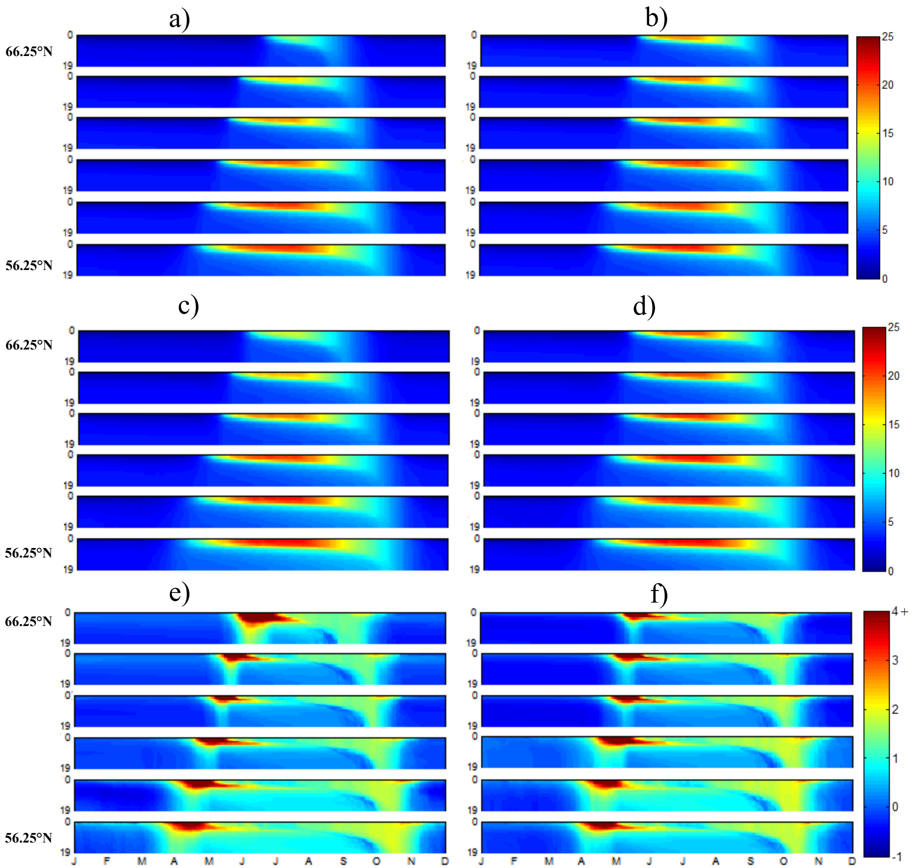

Fig. 13. Modeled mean daily lake-water temperature profiles during the 1961–1990 (**a** and **b**) and 2041–2070 (**c** and **d**) time periods as well as the corresponding changes between these periods (**e** and **f**) at 2° latitude intervals along 15° E (**a**, **c** and **e**) and 25° E (**b**, **d** and **f**) longitudes. Note that the temperature changes have been constrained to a maximum of 4 °C for better representation.

TCD
7, 743–788, 2013